Excited-State Behavior of trans and cis Isomers of Stilbene and Stiff Stilbene: A TD-DFT Study

R. Improta*,† and F. Santoro‡

Istituto di Biostrutture e Biommagini del CNR, via Mezzocannone 6, I-80134 Napoli, Italy, and Istituto per i Processi Chimico-Fisici del CNR, Area della Ricerca del CNR di Pisa, via Moruzzi 1, I-56124 Pisa, Italy

Received: August 1, 2005; In Final Form: September 9, 2005

The first part of the isomerization path on the two lowest excited states of trans and cis isomers of stilbene and stiff stilbene is investigated by means of TD-PBE0 calculations in the gas phase and in heptane solution. Solvent effects are taken into account by the PCM model. The excited-state optimized structures and the computed absorption and emission frequencies are in good agreement with the available experimental results. In all of the examined compounds, the isomerization process before barrier crossing occurs on the HOMO → LUMO bright state, whereas the role played by other single-excitation states appears negligible. The relative energy barriers on the isomerization paths are consistent with the experimental excited-state lifetimes, suggesting a unifying picture of the isomerization process in stilbene-like molecules.

Several computational papers published in very recent years[1−10] have allowed a remarkable advance toward a full understanding of the stilbene photoisomerization process, providing the ground for interpreting the quickly growing amount of experimental results concerning the photoexcited behavior of *trans*- and *cis*-stilbene.[11−14]

trans-Stilbene has been investigated more thoroughly, and the basic features of its lowest-energy singlet excited states (S_1, S_2) seem well assessed. The ground state (S_0) equilibrium geometry is planar (C_{2h} symmetry), although the phenyl rings can rotate with a very low energy cost.[15,16] All of the previous theoretical studies agree in predicting that there are three states that could be, in principle, involved in the excited-state dynamics following absorption in the range of 330−260 nm, corresponding to its absorption spectrum.[17,18]

The bright state corresponds to the highest occupied molecular orbital (HOMO) → lowest unoccupied molecular orbital (LUMO) transition (see Figure 1), yielding to a B_u state (hereafter B_{HL}). The second state, weakly absorbing, also has a B_u symmetry (hereafter B_-) and results mainly from a combination of local excitations on the phenyl groups, namely, from the antisymmetric combination of the quasidegenerate HOMO → LUMO+1 and HOMO−1 → LUMO configurations. The third state is A_g, dark by symmetry, and is mainly a combination of HOMO−2 → LUMO and HOMO → LUMO+2 excitations, and in the following will be labeled as 2*A*. Because of the shape of the orbitals involved in the excitations, 2*A* can be considered the symmetric counterpart of the B_- state. There is also a general consensus on the energy ordering of the above states in the Franck−Condon (FC) region, that is

$$B_{HL} < B_- \approx 2A$$

Actually, CASPT2 calculations predict that B_- is slightly more stable than the B_{HL} state.[1] However, recent multistate-CASPT2 calculations[2] restored the *traditional* energy ordering, although

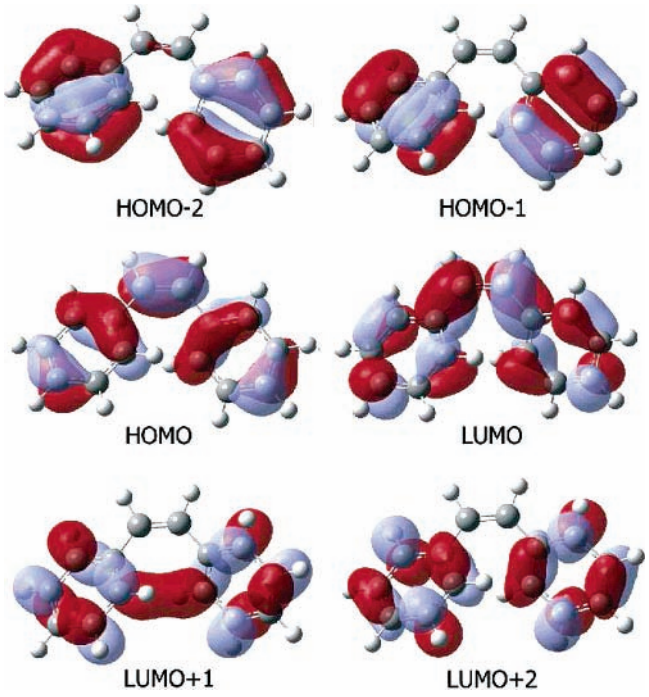

Figure 1. Isodensity plot of the *cis*-stilbene frontier molecular orbitals computed at the PBE0/6-31G* level of theory.

providing quite similar energies (3.86 and 4.17 eV) and intensities (0.49 and 0.32) for the B_{HL} and B_- states. Experimental spectra do not show mark for a second absorbing state, suggesting that the intensity of B_- should be much smaller than that of B_{HL}.[17]

It has been established clearly that the system must cross an energy barrier on the excited state along its photoisomerization path. The height of the barrier has been computed recently to be 750 cm^{-1} (1350 cm^{-1} before correction for zero point energies),[3] and this order of magnitude is compatible with the available experimental results.[19] After crossing the barrier, the system reaches pseudoperpendicular arrangements where the S_1 and S_0 states come close in energy and form a conical

* Corresponding author. E-mail: robimp@unina.it.
† Istituto di Biostrutture e Biommagini del CNR.
‡ Istituto per i Processi Chimico-Fisici del CNR.

10.1021/jp054250j CCC: $30.25
Published on Web 10/15/2005

intersection (CI). Although SA-2-CAS(2,2) calculations suggest that the CI is reached upon pyramidalization at one ethylenic carbon,[8] Fuss et al.[22] have recently demonstrated experimentally that it is formed through a hula-twist mechanism, in agreement with the prediction of molecular mechanics valence bond (MMVB) calculations.[6] At CI, the system makes a transition to S_0, producing a mixture of the trans and cis isomers. As pointed out by Orlandi et al.,[20] at pseudoperpendicular structures double excitations can significantly contribute to the lowest excited state. This is confirmed by the analysis of Fuss.[22]

The situation is less clear for *cis*-stilbene, which has been investigated less thoroughly by theoretical studies.[5,8] Because of steric hindrances, it exhibits a nonplanar C_2 S_0 equilibrium structure. CASPT2 calculations[5] predict that B_{HL} is the bright state, as in *trans*-stilbene, but corresponds to the $S_0 \rightarrow S_3$ transition, that is, there are two almost-dark states at lower energy. Specifically, the $S_0 \rightarrow S_1$ transition is predicted to lead to the B_- state, ~0.50 eV more stable than the B_{HL} state. Very recent pump−probe experiments have been interpreted on the ground of this state ordering by Fuss and co-workers.[20,21] After excitation to the B_{HL} state, an extremely fast (~25 fs) decay to the B_- state is postulated, where the system is assumed to vibrate in the minimum well before crossing the isomerization barrier.

However, as we have seen above, at least in *trans*-stilbene, CASPT2 computations have been shown to overestimate the stability of the B_- state. Furthermore, for *cis*-stilbene the good mirror image symmetry found between the absorption and emission spectra[23] would suggest that the absorbing and the emitting state coincide. This hypothesis seems to be in contradiction with the ultrafast nonradiative transition postulated by Fuss.[21] However, there are systems in which the assumption that this finding always implies that the emitting state is the lowest-energy one has been shown to be wrong.[24] To summarize, the excited state energy ordering in *cis*-stilbene cannot be considered firmly established.

The elucidation of the exact state ordering in the FC region is relevant not only for interpreting the excited-state dynamics of stilbene but also for understanding what physicochemical factors are responsible for the energy barriers on the S_1 state. In fact, according to the most accepted explanations, at least in *trans*-stilbene, this barrier arises from the interaction of the B_{HL} state with either the double-excited state[20] or with the B_- state.[1]

Additional information on the excited state of stilbene has been obtained by studying stilbene-like molecules modified properly. One of the most commonly investigated is 2,3,2′,3′-tetrahydro-[1,1′]-biindanylidene, shortly named hereafter as stiff stilbene or simply stiff (see Figure 2), concerning both its vertical transitions[17] and its trans → cis photoisomerization.[28,29] The same discrepancies found in the description of the *cis*-stilbene excited dynamics are found in stiff stilbene. In fact, also for this molecule, Fuss et al. have invoked the presence of a low-lying almost-dark state to give account of some results of pump−probe experiments on its trans isomer (*trans*-stiff).[22] However, according to the measurements of Hohlneicher et al.,[17] the bright B_{HL} is the lowest excited state in *trans*-stiff, whereas the weakly absorbing B_- state lies ~0.6 eV above it.

We therefore decided to reconsider the behavior of the lowest energy states of stilbene and stiff stilbene in detail. To this aim, we performed a density functional theory (DFT) and time-dependent DFT (TD-DFT) study of S_0, S_1, and S_2 in the gas phase and in apolar solution, focusing our attention on the first part of the isomerization path. By a critical comparison of our results with the available experimental data, our aim is to indicate what the most plausible excited-state energy ordering in the FC region is. Furthermore, we will monitor how the energy and the nature of the lowest excited states change during the first step of the photoisomerization process, that is, for θ in the range 0−60°, getting information on the initial excited-state dynamics. This will help to shed some light on the chemical−physical factors responsible for the presence of a barrier on the isomerization path. This study will give us the opportunity to reexamine the behavior of the trans isomers of stilbene and stiff stilbene, which we have studied previously at the TD-DFT level,[9,10] looking for a common and unifying description of the first part of the photoisomerization process in stilbene-like molecules, in which the role played by electronic and steric factors is critically evaluated. We will present equilibrium structures, relaxed paths as a function of the reactive torsion, and two-dimensional (2D) scans on the S_1 and S_2 surfaces, providing information that at the present level of theory is not available in the literature, to our knowledge. Actually, the task

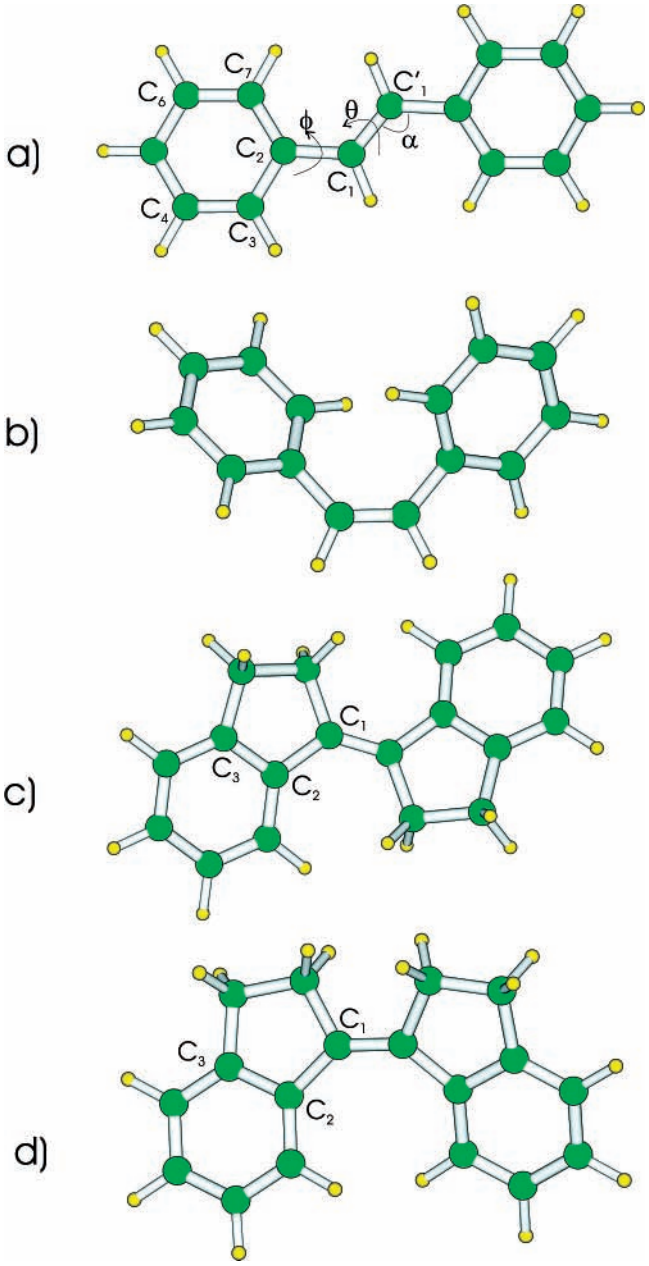

Figure 2. Schematic drawing and atom labeling of S_0 minima of the four compounds under study: (a) *trans*-stilbene (b) *cis*-stilbene (c) *trans*-stiff (d) *cis*-stiff.

TABLE 1: Main Geometrical Parameters of the S_0 (PBE0/6-31G(d) Geometry Optimizations), S_1, and S_2 (TD-PBE0/SV(P) Geometry Optimizations) Minima of *cis*-Stilbene[a]

	S_0		S_1[b]	S_2
	calcd	exptl[c]		
C1−C1′	1.346	1.334	1.417	1.390
C1−C2	1.470	1.489	1.412	1.432
C2−C3	1.402	1.398	1.428	1.418
C7−C2	1.403	1.398	1.447	1.424
α	130.4	129.5	124.8	127.4
C1−C2−C3	119.0		120.9	120.4
C6−C7−C2	120.7		120.3	117.2
C7−C2−C1	122.8		122.0	122.4
θ	−6.9		34.3	20.5
ϕ	35.0	43.0	11.6	21.8

[a] Bond distances in Å, bond angles and dihedral angles in degrees. [b] Phenyl hydrogen atoms are kept coplanar with the phenyl ring. [c] Gas-phase electron diffraction[40]

of exploring a large region of the potential energy surfaces (PES) of two excited states, together with the good results obtained previously on *trans*-stilbene, prompt us to resort to TD-DFT calculations. The well-known deficiencies of TD-DFT in treating double excited states and conical intersections, which would make any analysis of the phantom state less reliable, should not affect this study, which explores region of the PES where the weight of double excited states should not be relevant and with S_0/S_1 energy gaps larger than 2 eV.

1. Computational Details

In this work, we utilized DFT and TD-DFT methods,[30] employing the PBE0[31] functional provided by the Gaussian03 package,[32] except for excited-state optimization where we utilized the TURBOMOLE package.[33] Despite the absence of adjustable parameters, when employed in TD-DFT calculations, PBE0 (TD-PBE0) has already provided excitation spectra in very good agreement with the available experimental results.[9,34] Ground-state geometry optimizations have been performed with the standard 6-31G(d) basis set, whereas excited-state optimizations with TURBOMOLE utilize the SV(P) basis set, whose quality is comparable with that of the 6-31G(d) one.[33] All of the stationary points have been characterized by the vibrational frequency analysis, checking that the minima and the transition states exhibit zero and one imaginary frequency, respectively. The energies of the different states at the optimized structures have been refined adopting larger basis sets, 6-31+G(d,p) and 6-3111-G(2d,2p). Bulk solvent effects on the ground and the excited states have been taken into account by means of the polarizable continuum model (PCM).[36] In this model, the molecule is embedded in a cavity surrounded by an infinite dielectric, with the dielectric constant of the solvent (we have used *n*-heptane, dielectric constant 1.92). The cavity of the solute is defined in terms of interlocking spheres centered on nonhydrogen atoms, whose radii are optimized according to the UAHF model.[35] PCM/TD-PBE0 calculations have been performed according to the procedure outlined in ref 37.

Wiberg bond orders[38] have been calculated on the ground of the natural bond orbital (NBO) analysis.[39]

2. Results

2.1. Ground-State Absorption. The main parameters of the ground-state geometries computed at the PBE0/6-31G(d) level for *cis*-stilbene are reported in Table 1 (see Figure 2 for atom labeling; the optimized geometries for *cis*- and *trans*-stilbene can be found in the Supporting Information). In contrast to *trans*-stilbene, the steric hindrance between the phenyl rings causes a nonplanar C_2 equilibrium geometry for S_0 *cis*-stilbene, and the computed ϕ dihedral (35.0°) is close to those measured by gas-phase electron diffraction experiments (43.2°).[40] The remaining geometrical parameters are also in good agreement with the available experimental and previous computational results.[5] It is relevant for our following analysis that the large value of the α bond angle is predicted correctly.

TABLE 2: Main Geometrical Parameters of the S_0 (PBE0/6-31G(d) Geometry Optimizations) and S_2 (TD-PBE0/SV(P) Geometry Optimizations) Minima of *trans*-Stiff[a]

	S_0		S_2
	calcd	exptl[b]	
C1−C1′	1.353	1.349	1.407
C1−C2	1.468	1.470	1.440
C1−C2′	1.468	1.470	1.436
C2−C3	1.407	1.396	1.422
C7−C2	1.400	1.396	1.416
C3−C4	1.387	1.376	1.390
C7−C6	1.392	1.378	1.390
C3′−C4′	1.387	1.376	1.435
C7′−C6′	1.392	1.378	1.427
α	127.7	128.7	127.7
α′	127.7	128.7	128.1
C1−C2−C3	109.7	110.3	109.4
C6−C7−C2	119.2	118.5	119.0
C7−C2−C1	131.1	131.2	131.6
θ	178.9		174.9
ϕ	166.8	179.8	171.7

[a] Bond distances in Å, bond angles and dihedral angles in degrees. [b] From ref 41.

TABLE 3: Main Geometrical Parameters of the S_0 (PBE0/6-31G(d) Geometry Optimizations), S_1, and S_2 (TD-PBE0/SV(P) Geometry Optimizations) Minima of *cis*-Stiff[a]

	S_0		S_1	S_2
	calcd	exptl[b]		
C1−C1′	1.352	1.335	1.423	1.404
C1−C2	1.470	1.466	1.414	1.433
C2−C3	1.406	1.396	1.427	1.432
C7−C2	1.399	1.396	1.426	1.401
α	131.8	129.3	125.5	130.9
C1−C2−C3	109.4	110.3	110.2	108.0
C6−C7−C2	119.5	119.9	118.1	122.3
C7−C2−C1	131.0	131.2	129.7	129.5
θ	9.2		43.1	25.3
ϕ	20.5		5.2	14.8

[a] Bond distances in Å, bond angles and dihedral angles in degrees. [b] From ref 42.

From the energetic point of view, *cis*-stilbene is predicted by PBE0/6-311+G(2d,2p)//PBE0/6-31G(d) calculation to be less stable than the trans isomer by 4.42 kcal/mol (in the gas phase) and 4.60 kcal/mol (in heptane). These values are in very good agreement with the ΔH measured in apolar solvent (4.59 ± 0.09 kcal/mol).[5] This is a comforting result that supports the reliability of our computational approach in reproducing the subtle balance of steric hindrances and delocalization effects on the relative energy of stilbene isomers. By comparison, the energy difference computed in vacuo at the CASPT2 level is only 0.10 kcal/mol,[5] whereas CASSCF results are in good agreement with the experiment.[5,8]

The main parameters of the computed equilibrium geometry of *cis*- and *trans*-stiff stilbene are reported in Tables 2 and 3 (see the Supporting Information for the optimized geometries). For both compounds, they are close to that determined by X-ray

TABLE 4: Vertical Excitation Energies (in eV) Calculated by TD/PBE0 Calculations on the Geometries Optimized in the Gas Phase at the PBE0/6-31G(d) Level[a]

	6-31+g(d,p)		6-311+G(2d,2p)			
					heptane	
	trans	cis	trans	cis	trans	cis
			stilbene			
B_{HL}	3.98(0.93)	4.12(0.37)	3.94(0.91)	4.09(0.36)	3.84(1.04)	4.04 (0.44)
B_-	4.65(0.02)	4.66(0.00)	4.60(0.03)	4.61(0.00)	4.60(0.03)	4.61 (0.00)
$2A$	4.67(0.00)	4.90(0.00)	4.62(0.00)	4.87(0.00)	4.62(0.00)	4.87(0.00)
			stiff stilbene			
B_{HL}	3.87(0.82)	3.71(0.51)	3.83(0.80)	3.67(0.49)	3.74(0.94)	3.60(0.59)
$2A$	4.42(0.00)	4.48(0.01)	4.38(0.00)	4.45(0.01)	4.38(0.00)	4.44(0.02)
B_-	4.53(0.06)	4.50(0.05)	4.53(0.05)	4.46(0.05)	4.52(0.05)	4.46(0.06)

[a] Oscillator strength is given in parentheses.

diffraction.[41,42] Because of the geometrical constraints of the ethylenic bridge, the ϕ and ϕ' dihedrals in *cis*-stiff (as that of *trans*-stiff) are closer to planarity than in *cis*-stilbene; however, in agreement with experiments, a not negligible departure from planarity is predicted.

The optimized geometries have been used to compute (see Table 4) the vertical excitation energies (VEE) of *cis*-stilbene and *cis*-stiff by means of TD-PBE0 calculations in the gas phase and PCM/TD-PBE0 calculations in heptane. For comparison, the results obtained for the trans isomers at the same level of theory are also reported.

TD-PBE0 calculations provide a description of the lowest energy states of *cis*-stilbene, which are very similar to those we have found previously for *trans*-stilbene.[9,10] It is predicted that the lowest energy transition is strong and leads to the B_{HL} state. In agreement with experimental results, the relative absorption is less intense and significantly blue-shifted with respect to the corresponding band in *trans*-stilbene (~0.1−0.2 eV). The blue-shift is probably due to the larger deviation from the planarity of the phenyl substituent. Because of the shape of the frontier orbitals, rotation of the phenyl substituents increases the stability of the HOMO and decreases that of the LUMO, leading to a larger HOMO → LUMO transition energy.

According to our calculation, the $S_0 \rightarrow S_2$ transition is very weak and ~0.5 eV blue-shifted with respect to the $S_0 \rightarrow S_1$ one. As in *trans*-stilbene, it corresponds to the B_- state.

Finally, S_3 is the $2A$ state described above, even if there are additional, although small, contributions from different excitations. At the FC point, in *cis*-stilbene S_3 is less stable by ~0.25 eV than S_2, whereas in *trans*-stilbene these two states are almost degenerate. The reason is that in *cis*-stilbene LUMO+1, involved in the transition to S_2, is stabilized by a bonding interaction between the two phenyl rings, absent in LUMO+2, involved in the transition to S_3 (see Figure 1).

A quantitative comparison with the experiments is not easy because the experimental band is broad and structureless, with a maximum around 4.45 eV, that is, ~0.4 eV blue-shifted with respect to our computed VEE. Part of this discrepancy is surely due to the rotation of the phenyl rings, which is very easy in S_0 but requires a much higher energy expense in B_{HL} (see below). In fact, as we show in the next section, when one compares the 0−0 transition energy, not dependent on thermal distributions, the agreement with experiment is better with a difference of ~0.2 eV.

Considering stiff stilbene, the nature and the energy of the electronic transitions are very similar in the cis and trans isomer because of the fact that they are both planar in S_0. The energy ordering at the FC point for the two isomers is the same, that is., $B_{HL} < 2A \approx B_-$ and the intensity of the B_- transition is larger than that in stilbene, in agreement with the fact that it has been detected experimentally for *trans*-stiff.[17] From the quantitative point of view, the most remarkable difference between *cis*-stiff and *cis*-stilbene concerns the transition to B_{HL}: in *cis*-stiff, in agreement with experiments, it is red-shifted with respect to *trans*-stiff. This result is probably due to the interaction with the axial CH bonds of the vicinal methylenic group, which stabilizes the LUMO slightly and destabilizes the HOMO. In the cis isomer, this interaction is expected to be stronger because the CH bond is closer to being perpendicular to the ethylene plane (i.e., better aligned with the π system), and, as a consequence of the interaction, the CH bond length is slightly longer.

To summarize, our computational approach gives a picture in good agreement with the available experimental results. From the quantitative point of view, both the differences between the cis/trans isomers and the effect of the saturated bridge (in stiff stilbene) on the VEE are very well reproduced, whereas the error on the absolute VEE is ~0.2 eV, except for the case of *cis*-stilbene, where the larger error is probably motivated by thermal effects, as discussed above.

Concerning the ordering of the states in *cis*-stilbene, the broadness of the absorption spectra do not allow one to unambiguously ascertain if the energy order predicted by TD-PBE0 calculations is correct. In addition, the lack of accurate absorption spectra for *cis*-stiff avoid the possibility to directly test the reliability of TD-PBE0 as was done for *trans*-stilbene. For this isomer, the picture provided by TD/PBE0 corresponds fully to the experimental one. In fact, for *trans*-stilbene it predicts the presence of a single strong peak (B_{HL}) in the range of 3.5−4.8 eV, whereas the B_- and $2A$ transitions, both with an energy of ~4.7 eV, have vanishing oscillator strengths. Only one strong transition is indeed detectable in the UV−Vis spectra under 4.8 eV, and its position is in good agreement with our computed value. In *trans*-stiff, instead, the B_- transition has a larger oscillator strength than its counterpart in *trans*-stilbene, and in fact experimental spectra show the presence of a weak band ~0.7 blue-shifted with respect to the strong absorption peak around 3.8 eV,[17] and TD-PBE0 results agree nicely with experiments in this case also.

As a final remark, it is worthwhile to notice that the adoption of PCM allows one to predict a solvent red shift on the absorption maxima in good agreement with the experimental data (0.2 eV, see the discussion in our previous work[9]), confirming the usefulness of suitable continuum models for describing solvent effects on electronic spectra.

2.2. Excited-State Potential Energy Surface. To describe the first steps along the isomerization path, we have performed a relaxed TD-PBE0//TD-PBE0/SV(P) scan of the excited (PES)

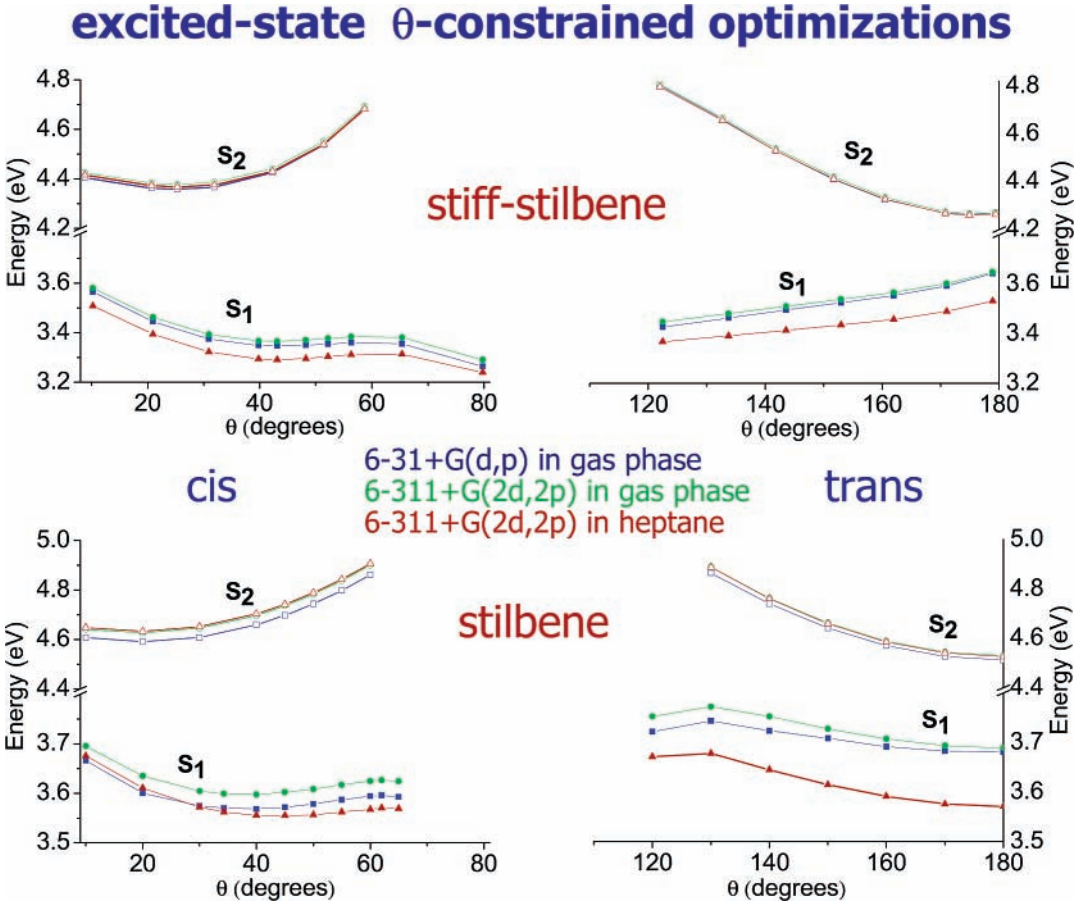

Figure 3. S_1 and S_2 energy profiles for both isomers of stilbene and stiff stilbene obtained by TD-PBE0/SV(P) partial optimizations at fixed θ dihedrals. Energies are reported in the gas-phase (squares and circles, for the 6-31+G(d,p) and the 6-311+G(2d,2p) basis set, respectively) and in *n*-heptane (triangles, 6-311+G(2d,2p) basis set).

S_1 and S_2 as a function of the θ dihedral, which is varied between 0° and ~65°. Figure 3 reports the paths for both isomers of stilbene and stiff stilbene.

***cis*-Stilbene**. The S_1 (B_{HL}) curve for *cis*-stilbene has been built imposing that phenyl hydrogen atoms H_3 and H_3' are coplanar to the phenyl rings. Without this constraint, a TD-PBE0 geometry optimization starting from the FC structure (i.e., the S_0 equilibrium geometry) deforms the molecule in the direction of the ring closure leading to dihydro-phenantrene (DHP), with a progressive narrowing of the S_1/S_0 energy gap that indicates the approach to a conical intersection that cannot be characterized at the TD-DFT level. A detailed characterization of this conical intersection was presented at the MMVB level of theory,[6] and in agreement with those results, our calculations suggest that pyramidalization of the C_7/C_7' atoms together with rotation of dihedrals φ and φ' and the closure of the α and α′ angles play the most relevant role in the first steps of this photocyclization process.

The B_{HL} state at the PBE0/SV(P) level exhibits a shallow C_2 minimum at $\theta = 34.3°$, see Table 1, which increases to ~40.0° when refining the energies with larger basis sets (see Figure 3). TD-PBE0 predicts that this structure is unstable with respect to the out-of-plane motion of the phenyl. However, the analysis of Raman resonant (RR) experiments predicts a minimum of the *emitting* state with $\theta = 37°$.[43] Furthermore, the computed 0−0 excitation energy and fluorescence energy (see Table 5) are in good agreement with the results obtained by fitting the experimental spectra[43] (within 0.2 eV). Those evidences support the idea that B_{HL} is the emitting state in *cis*-stilbene and that the pseudominimum on the curve of Figure 3 is representative of a real minimum or, at least, of a metastable species.

TABLE 5: Experimental and Calculated 0−0 Transition and Fluorescence Energy (in eV) for trans and cis Isomers of Stilbene and Stiff Stilbene

	0−0 transition energy calculated			
	6-31+G(d,p)	6-311+G(2d,2p)		
	gas phase	gas phase	heptane	exptl
stilbene				
trans	3.68	3.69	3.57	3.81,[a] 3.85[b]
cis	3.39[c]	3.41[c]	3.36[c]	3.57[d]
stiff				
trans				3.65,[a] 3.66[b]
cis	3.22	3.23	3.16	3.52[a]
	fluorescence maxima calculated			
	6-31+G(d,p)	6-311+G(2d,2p)		exptl
	gas phase	gas phase	heptane	
stilbene				
trans	3.39	3.35	3.24	~3.50[e], 3.71[b]
cis	2.48[c]	2.45[c]	2.41[c]	~2.85[f]
stiff				
trans				3.60[b]
cis	2.39	2.36	2.29	

[a] In 3MP[17]. [b] In *n*-hexane[56]. [c] Estimated, S1 minima with hydrogen planar. [d] From a fitting of the experimental spectrum[43]. [e] In *n*-hexane[29]. [f] In *n*-hexane[44].

Beyond the twist at the θ dihedral, the main change with respect to the S_0 equilibrium structure involves the φ and φ'

torsions that move toward planarity, the α and α′ bond angles that become sensibly narrower (∼6°), and the C_1-C_1' and $C_1-C_2/C_1'-C_2'$ bond lengths that decrease and increase, respectively, by about 0.06 Å. Significant but minor changes also take place on the benzenic bonds, and all are easily understandable by looking at the difference of the HOMO and LUMO orbitals (see Figure 1) involved in the S_0/S_1 transition.

At θ larger than the minimum value, the B_{HL} curve retains the C_2 symmetry and slowly increases up to $\theta = 62°$. After this point, the energy of the state drops and TD-PBE0 geometry optimizations suffer from severe convergence problems, probably because of the proximity of the S_1/S_0 CI. Nevertheless, a partially relaxed single-point calculation for $\theta = 65°$ confirms that the energy of B_{HL} decreases with respect to $\theta = 62°$, suggesting that this point is a saddle point on the isomerization path. The estimated energy barrier is in the range of 100−200 cm^{-1}, depending on the basis set size and on the inclusion of solvent effects. These values are consistent with the experimental estimates of the energy barrier that are in the 0−400 cm^{-1} range.[25−27] It is important to notice that, because of the large geometry shift associated with the $S_0 \rightarrow B_{HL}$ transition, after excitation the *cis*-stilbene is vibrationally hot. As a consequence, it is not surprising that some experimental studies predict that the photoisomerization path would be barrierless in the gas phase.[44]

Also, the curve on S_2 preserves the C_2 symmetry (B_- state) (see Figure 3). It is rather different from that seen on B_{HL}. As expected, rotating the θ angle causes the energy of B_- to increase more steeply, indicating a much larger barrier to the isomerization. This is due to the fact that the double-bond character of the C_1-C_1' bond decreases less in B_- than in B_{HL}. This feature also explains why the B_- minimum is found at $\theta = 20.5°$, significatively less rotated than the B_{HL} one. In addition, the shifts along the other coordinates with respect to the S_0 equilibrium structure are less pronounced than they are for the B_{HL} minimum. The computed fluorescence maximum from B_{HL} is significantly lower (about 0.45 eV) than the experimental estimate, an error very similar to that reported for the maximum absorption spectrum. As a consequence, our calculations match the experimental Stokes shift (exptl ∼1.6 eV, computed 1.63 eV) almost perfectly.

***trans*-Stilbene**. Full-relaxed excited-state geometry optimizations allow one to locate an energy minimum on both the S_1 and S_2 states (see the Supporting Information). For S_1 (B_{HL}), the predicted geometry is planar (C_{2h} symmetry) and similar to that obtained at a more approximate level, as discussed already in our previous paper.[10] With respect to those predictions, a difference is seen for S_2 because by relaxing the C_2-symmetry constrain a C_1 global minimum is found (see the Supporting Information for detailed data), although at the TD-PBE0/SV(P) level it is only 1.1 kcal/mol more stable than the C_2 one. It corresponds to the M_{benz} minimum obtained by MMVB theory[6] and is probably due to the interaction between the almost degenerate B_- and 2A states. The 0−0 excitation and fluorescence energies found for the B_{HL} minimum are in good agreement with the available experimental data: they are underestimated by ∼0.2 eV in line with the discrepancy found for the VEE. This result not only confirms that B_{HL} is the emitting state in *trans*-stilbene but further supports the reliability of our computational approach.

According to our previous partial TD/PBE0 geometry optimizations,[10] an energy barrier is also predicted for the photoisomerization of *trans*-stilbene. Its value on B_{HL} is predicted to be in the 500−850 cm^{-1} range, somewhat underestimated with respect to previous computational studies (which report a value of 750 cm^{-1} after correction for the zero-point energy, which tends to lower the barrier). The comparison of the results between cis and trans isomers is consistent with the available experimental results that show a much slower photoisomerization in *trans*-stilbene than in *cis*-stilbene.[11,45]

Stiff Stilbene. In Figure 3, we report the relaxed path on the S_1 and S_2 surfaces of *cis*- and *trans*-stiff as a function of the θ dihedral. Although a C_1 path collapses on C_2 structures on S_1 and can thus be labeled with the C_2 symbol B_{HL}, the path remains C_1 on S_2. The closeness of the S_2 and S_3 states for both isomers confirms that the loss of the C_2 symmetry, also seen in *trans*-stilbene but not in *cis*-stilbene, can be ascribed to a $B_-/2A$ interaction. The computed curves for both isomers of stiff stilbene are qualitatively more similar to those obtained for *cis*-stilbene than for *trans*-stilbene. For *cis*-stiff, because of the presence of the saturated cycle, the pathway analogue to that leading to DHP in *cis*-stilbene is not easily accessible. As a consequence, a shallow true-minimum is found on the B_{HL} curve, without imposing any geometry constraint (see Table 3). Table 5 shows a good agreement between the computed 0−0 and the available experimental results, supporting the reliability of our computational approach. Because of the similarity in the nature of the electronic excitations, it is not surprising that the most relevant geometry changes caused by the $S_0 \rightarrow B_{HL}$ transition (see Table 3) are similar to those found for *cis*-stilbene. Also, for *cis*-stiff a small barrier on the isomerization path of B_{HL} is predicted, but its value is estimated in the 50−100 cm^{-1} range, that is, even smaller than that predicted for *cis*-stilbene. For *trans*-stiff the minimum on B_{HL} disappears, and consequently the barrier also vanishes, in line with the lifetime of the excited state shorter than that in *cis*- and *trans*-stilbene.[21]

As found for stilbene, the isomerization path on S_2 appears unfeasible because by twisting θ the energy increases steeply. This is true on both the fully relaxed C_1 paths shown in Figure 3 and on C_2 constrained paths, directly associable to the B_- state, which are slightly higher in energy and are not shown for lack of space.

2.3. Initial Motion on the Excited Surface of *cis*-Stilbene. To gain more insight on the motions involved in the initial dynamics of *cis*-stilbene after the excitation, we computed several 2D scans of S_1 and S_2 at the TD-PBE0/6-31G(d) level, varying two coordinates and freezing all of the others to the values of the FC structure. We considered the θ, φ, φ', α, and α′ coordinates. In Figure 4, we report the contour lines of the S_0, S_1, and S_2 surfaces for the C_2-symmetry scans (θ, φ), (φ, α), and (α, θ), where for the symmetry constrain $\alpha' = \alpha$ and $\varphi' = \varphi$. Notice that to better put minima and barriers into evidence the contour lines have a variable spacing, as indicated by the energy values on the isopotential curves. The FC point is indicated by a black spot. It is important to stress that the closely lying S_2 and S_3 (adiabatic) states, at the present level of theory, do not preserve the same symmetry character (A or B) at all of the scanned nuclear structures. On the contrary, they exchange the symmetry character, suggesting that crossing occurs between the corresponding diabatic (symmetry preserving) states and that nonadiabatic effects can be important in the nuclear dynamics on these states.

2D (φ, θ) scan. The S_0 surface is very anharmonic along the φ coordinate and is much flatter toward values larger than the equilibrium one (FC point) than toward smaller values. An increase of φ from 35° to 50° costs ∼0.1 eV on S_0, ∼0.5 eV on S_1, and ∼0.4 eV on S_2, supporting the fact that thermal effects increase the absorption maximum. The S_2 surface appears bound

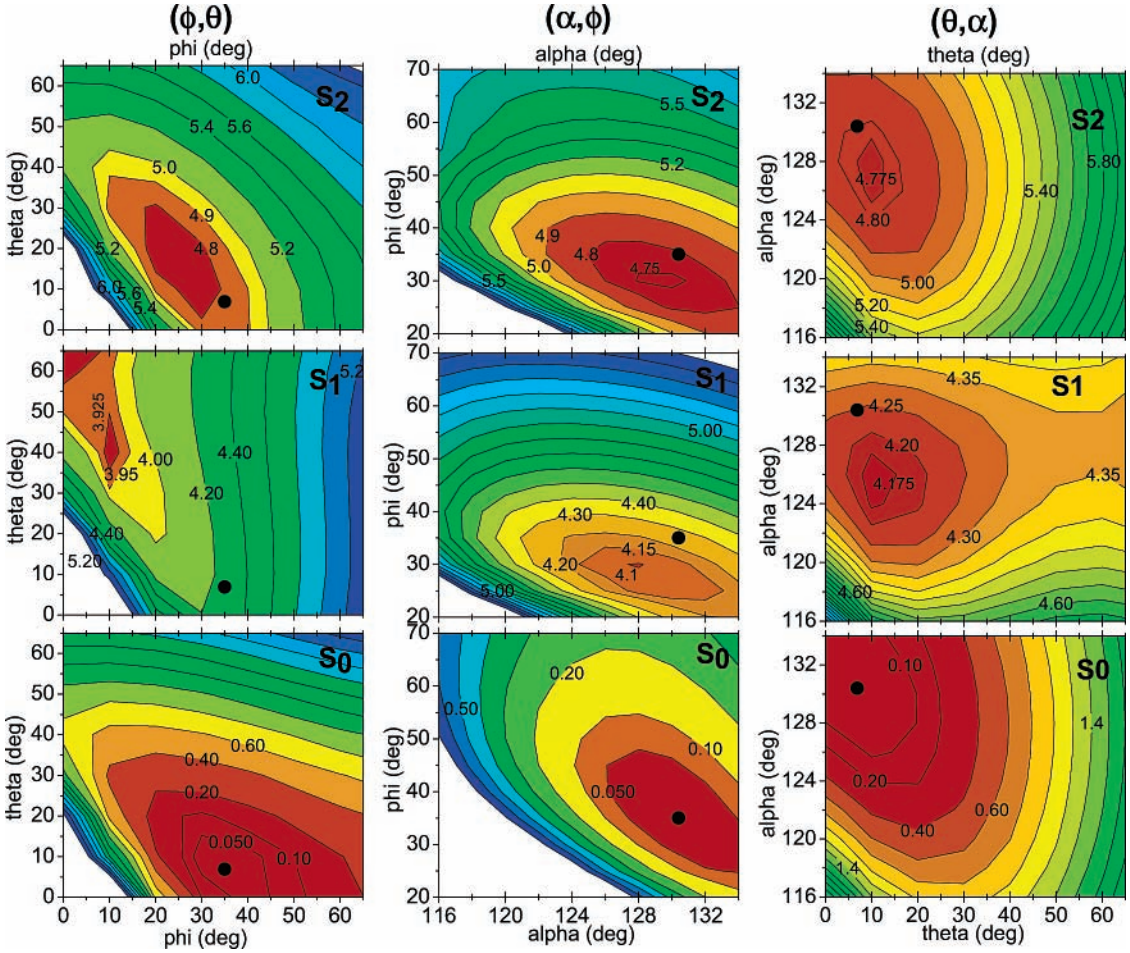

Figure 4. Two-dimensional C_2-symmetry scans of the S_0 (bottom), S_1 (central), and S_2 (upper) *cis*-stilbene electronic surfaces, obtained at the TD-PBE0/6-31G(d) level varying two coordinates and freezing all of the others to the FC structure values. Left panels: (φ, θ) scan ($\varphi' = \varphi'$); central panels: (α, φ) scan ($\alpha' = \alpha', \varphi' = \varphi'$); right panels ($\theta$, α) scan ($\alpha' = \alpha'$)

and unreactive (considering the energy of the FC point, the system cannot twist to more than $\theta \approx 40°$). On the contrary, on the S_1 surface it is evident that by a coupled $\theta-\varphi$ motion the system can reach a shallow minimum and, after crossing a very small barrier, it can twist further the θ angle approaching a pseudoperpendicular arrangement. Here the system should find the S_1/S_0 conical intersection, which is not computable with the TDDFT approach.

2D (α, φ) Scan. The 2D scans show that these two motions are clearly coupled on all three surfaces. As in previous scans, the S_0 surface appears very flat for twisting the φ angle toward values larger than that of the FC structure. From such a structure, the coupled motion appears to have a larger amplitude on S_1 than on S_2 (compare the region spanned by the contours at 4.8 eV on S_2 and at 4.3 eV on S_1 where the FC point approximatively resides). As specified above, in the scan reported we imposed $\Delta\varphi = \Delta\varphi'$ and $\Delta\alpha = \Delta\alpha'$, thus constructing two *a*-symmetry coordinates that preserve the C_2 symmetry of the FC structure. We also performed a different scan along *b*-symmetry coordinates defined by $\Delta\varphi = -\Delta\varphi'$ and $\Delta\alpha = -\Delta\alpha'$, which removes the molecular C_2 symmetry. These results (not reported for lack of space) show that from the FC structure there is no driving force to remove the C_2 symmetry along these coordinates on either the S_1 or S_2 surface.

2D (θ, α) Scan. These plots put in better evidence why the motion along α is expected to have a wider amplitude on S_1 than on S_2 because on the former surface the larger shift of the equilibrium position with respect to the FC structure is apparent. Once more, the θ twisting appears much more constrained on S_2 than on S_1, where in any case a barrier is seen. Notice that this barrier is not the lowest barrier for twisting θ, which is reached by a simultaneous motion along the φ and φ' coordinates (see the left column of Figure 4).

3. Discussion

3.1. Energy Barrier on the Photoisomerization Path. As we have discussed in Section 2.3, TD-PBE0 computations predict the existence of a barrier to the photoisomerization on S_1 (B_{HL}) for both stilbene and stiff stilbene. Its height decreases going from *trans*-stilbene (500−850 cm^{-1}) to *cis*-stilbene (130−230 cm^{-1}), to *cis*-stiff (50−150 cm^{-1}), and finally to *trans*-stiff (no barrier). The relative heights are in full agreement with the experimental measures of the times needed to overcome them, which are several ps (depending on the excited wavelength)[46,47] for *trans*-stilbene, ∼300 fs for *cis*-stilbene,[21] and ∼180 fs for *trans*-stiff.[22] As noted above, the absolute height of the barrier for *trans*-stilbene is probably underestimated, and the same could happen for the other cases (in particular, a very small barrier is also plausible for *trans*-stiff).

Because TD-PBE0 reproduces the energy barriers semiquantitatively, it is possible to put forward some hypothesis on their physical nature. The B_{HL} state always corresponds to the lowest energy transition, and its nature does not change significantly before reaching the saddle point. The transition always has a dominant, though slightly decreasing, HOMO → LUMO character. The weight of different excitations is always smaller

than 0.1 and, at this level of theory, there is no indication that the barrier is due to the interaction with an upper electronic state. In particular, because TD-DFT does not consider double excitations, the barrier it found cannot be explained by the interaction with the double-excited state invoked by Orlandi.[20]

Therefore, the presence (or absence) of the barrier seems to be mainly an *intrinsic* feature of the B_{HL} state, although its height can of course be modulated by the interaction with other states. Actually, in stilbene-like molecules both the HOMO and the LUMO are not fully localized on the central ethylenic moiety but receive significant contributions from the phenyl rings. As a consequence, in contrast with ethylene, C_1-C_1' bonds retain a significant double-bond character in the B_{HL} state. At the S_0 equilibrium geometry, for example, *cis*-stilbene exhibits a Wiberg bond index equal to 1.82 in S_0, 1.38 in B_{HL}, and 1.57 in B_-. For comparison, in the ground electronic state, the Wiberg bond index between bonded carbon atoms in the phenyl rings is ~1.4. However, in the B_{HL} minimum the C_1-C_1' bonds is ~1.41 Å, suggesting a partial double-bond character, which would explain the presence of a barrier on the isomerization path. Interestingly, because of the larger steric repulsion C_1-C_1' bond orders in both isomers of stiff stilbene are smaller, as mirrored by the longer bond distances. As an example, in *cis*-stiff Wiberg bond index is 1.59 already in the S_0 state and becomes 1.21 on B_{HL}, suggesting a smaller barrier for the isomerization.

The interplay between the residual double-bond character (preferring a planar arrangement) and the steric hindrances between the phenyl substituents (preferring a perpendicular arrangement), besides influencing the C_1-C_1' bond strength, represents the cause of the barrier to the isomerization at the TD-DFT level of theory. Furthermore, the barrier height is different in the four compounds examined as a result of the different steric hindrances they suffer. In *trans*-stilbene these are much smaller than those in *cis*-stilbene, and the former compound indeed exhibits the largest barrier. On the contrary, highly sterically hindered *cis*- and *trans*-stiff exhibit a very small, if not vanishing, barrier.

3.2. Interpretation of the Excited-State Pump−Probe Experiments on *cis*-Stilbene. Our computations allow us to comment on the results of the pump−probe experiments of Fuss et al.[21,22] on *cis*-stilbene, with a pump at 270 nm (4.6 eV), and probes of different carrier frequency (810 or 2100 nm) that induce a multiphoton ionization of the molecule. These measurements indicate that, after the excitation, the wavepacket oscillates with two main frequencies, 240 and 56 cm^{-1}, and cross the barrier in the θ-twisting direction in ~300 fs. By comparison with previous experiments,[48] the oscillations were assigned to motions along α, coupled with some φ component (240 cm^{-1}) and along φ (56 cm^{-1}). On the basis of the CASPT2 results of Molina et al.,[5] which identify the strongly absorbing B_{HL} state with the S_3 state, the authors assume that the initial excitation is on S_3. They postulate the occurrence of an ultrafast $S_3 \rightarrow S_1$ transition and that the observed periodic vibrations take place on the S_1 (B_-) surface before crossing the barrier toward $\theta = 90°$.

The existence of such a $S_3 \rightarrow S_1$ transition cannot be considered certain because on one hand it must be so fast (<25 fs) to be not detected and, on the other hand, the authors state that its introduction worsens the quality of the fits of their experimental data. Our results suggest a different interpretation of their data. The pulse at 4.6 eV excites *cis*-stilbene almost exclusively on the B_{HL} state (the others states are almost dark), which, according to TD-DFT, is the S_1 state. After excitation, the system stays on the B_{HL} surface and can follow two pathways[49−51] (i) a decay toward a conical intersection leading to DHP or (ii) a coupled motion along θ and φ toward the stationary point reported above on the B_{HL} curve. From this structure, after crossing a small energy barrier (130−230 cm^{-1}), it can further twist the θ angle and reach pseudoperpendicular arrangements where it accesses the S_1/S_0 conical intersection responsible for the cis−trans photoisomerization. The 300-fs time, indicated by Fuss et al.[21,22] as the time for crossing the barrier along path ii, agrees much better with the small barrier we found on B_{HL} than with the steep increase of the energy documented for B_- at the twist of θ. This supports our thesis that the barrier crossed is indeed on B_{HL}.

Experimental data indicate a 0.1 yield of DHP, a 0.35 yield of trans isomer, and a 0.55 yield of recovery of reactant.[52] Because TD-PBE0 free optimization from the FC structure leads directly onto the DHP-formation channel, these data suggest that either TD-DFT fails to see an existing barrier to DHP or that the cis → trans process is favored by a pure dynamic factor, determined by the wavepacket initial acceleration and the kinetic energy it can acquire in the dynamics. Actually, as shown by the 2D scans in the previous section, the initial acceleration surely has a component along the coupled $\theta-\phi$ motion leading toward the barrier to isomerization.

Concerning the vibrations observed by Fuss,[21] our 2D scans suggest that an FC wavepacket will oscillate along α and ϕ (preserving a C_2 symmetry) both on the S_2 and on the $S_1(B_{HL})$ surface, but with larger amplitudes on the latter surface. This finding, confimed by experiments,[53] further supports the idea that the motion in the first 300-fs window after the pulse is entirely on the $S_1(B_{HL})$ surface.

The interpretation proposed here allows one to avoid the assumption of the extremely fast (B_{HL}/B_-) (S_3/S_1 according to CASPT2) transition. TD-PBE0 results suggest that such an ultrafast transition is unlikely because the B_{HL} and B_- states are well separated in energy (with the former being the more stable) along the preferential path followed by the system right after the excitation on B_{HL} (see Figure 4).

Considering *trans*-stiff, investigated by the same authors in ref 22, the picture suggested by TD-DFT is similar. However, for this molecule the barrier on B_{HL} is smaller (according to TD-PBE0 vanishingly small) and thus the system twists more quickly than in *cis*-stilbene (in ~180 fs, according to Fuss).[22] The subsequent dynamics toward the conical intersection is slower as witnessed by the experimental decay time (~800 fs).

If the isomerization takes place directly on the B_{HL} state both for *cis*-stilbene and *trans*-stiff, then the nature of the process leading to the 150-fs decay time observed by Fuss[22] in *trans*-stiff and ascribed to the $B_{HL} \rightarrow B_-$ transition remains to be explained. In this respect we notice that: (i) the B_- state in trans-stiff has a larger oscillator strength than that in *cis*-stilbene and the exciting wavelength at 270 nm (4.6 eV) provides enough energy to excite it (the experimental $S_0 \rightarrow B_-$ band is at 4.29 eV, indeed),[17] (ii) femtosecond photoelectron spectroscopy of *trans*-stilbene excited at 266 nm gives rise not only to a 19-ps decay because of the isomerization process but also to a much faster decay with a time constant of ~100 fs.[10] This latter decay has been interpreted as coming from the excitation of the B_- state, which then decays toward the $2A$ or the B_{HL} states. An analogous explanation is also plausible for the signal decaying with 150 fs in *trans*-stiff, where, for example, the effect of the

$2A/B_-$ interaction is already evident in the loss of the C_2 symmetry of the S_2 equilibrium structure (see the previous sections).

4. Concluding Remarks

On the basis of the present computational results and the available experiments, several arguments strongly suggest that the dynamics after the optical excitation of *cis*-stilbene until the barrier crossing involves only the S_1 B_{HL}: (1) In contrast to B_{HL}, the large energy barrier on B_- is not compatible with a fast photoisomerization process. Moreover, the relative height of the barriers found on B_{HL} are in qualitative agreement with the experimental excited-state lifetimes (see the previous section). (2) The analysis of the excited-state stationary points and the 2D energy surface for *cis*-stilbene shows that B_{HL} is fully compatible (more than B_-) with the observed vibrational features, namely, the oscillation with frequencies 240 and 56 cm^{-1}. (3) The good mirror symmetry of the absorption and the emission spectra suggests that the absorbing and emitting state are the same. (4) A possible additional relaxation step, $B_{HL} \rightarrow B_-$, in *cis*-stilbene soon after the electronic excitation worsens the quality of the fit of the experimental data, as reported by Fuss et al.[21] and should be very fast ($\leq$25 fs) because it is not detected experimentally. This requires the existence of a conical intersection very close to the FC region. TD-DFT results do not see indications for such a conical intersection and indeed suggest that it is not necessary to postulate its existence.

Our computations concerning *trans*-stilbene and stiff stilbene are also in good agreement with the available experimental results, providing a unifying picture to the photoisomerization path of trans and cis isomers of stilbene and stiff stilbene, consistent with the experimental determination of the energy barrier and of the excited-state lifetimes. In all of the examined compounds, the first part of the isomerization path (i.e., for twisting of θ up to $\sim$50°) occurs on the B_{HL} bright state, whereas the subtle balance between electronic and steric factors rules the different energy barrier and, thus, the different photoisomerization time. A careful analysis of the effect of different substituents[54] on the height of the barrier could further validate this picture and will be addressed in a future work.

Obviously, the intrinsic limitations of TD-DFT do not allow one to get reliable information on the behavior for strongly twisted geometries, where the role played by double-excited states should be relevant. This lack could also lead to underestimate the energy barrier for the isomerization path because for $\theta \approx 60°$ an electronic interaction between the B_{HL} and the double-excited state might be possible.

It will thus be very interesting to further check the accuracy of our computations by using methods more sophisticated than TD-DFT. Unfortunately, the ordering of states provided for stilbene by the usually more reliable CASPT2 method is not in agreement with the available experimental results, suggesting the use of MS-CASPT2. However, a thorough exploration of the PES of the three lowest excited states of stilbene and stiff stilbene at this level of theory is computationally very expensive, making the very recent attempts of including double excited states within TD-DFT interesting.[55]

Supporting Information Available: Tables with the Cartesian coordinates of the different minima located on S_0, S_1, and S_2 surfaces for cis and trans isomers of stilbene and stiff stilbene. This material is available free of charge via the Internet at http://pubs.acs.org.

Acknowledgment. This work was supported by the Italian Ministry for the University and the Scientific Research (MIUR). We thank Professor W. Fuss and Professor G. Hohlneicher for very useful discussions and remarks.

References and Notes

(1) Molina, V.; Merchàn M.; Roos, B. O. *J. Phys. Chem. A* **1997**, *101*, 3478.
(2) Gagliardi, L.; Orlandi, G.; Molina, V.; Malmqvist, P.-Å.; Roos, B. O. *J. Phys. Chem. A* **2002**, *106*, 7355.
(3) Leitner, D. M.; Levine, B.; Quenneville, J.; Martinez, T. J.; Wolynes, P. G. *J. Phys. Chem. A* **2003**, *107*, 10706.
(4) Schroeder, J.; Steinel, T.; Troe, J. *J. Phys. Chem A* **2002**, *106*, 5510.
(5) Molina, V.; Merchàn, M.; Roos, B. O. *Spectrochim. Acta, Part A* **1999**, *55*, 433,
(6) Bearpark, M. J.; Bernardi, F.; Clifford, S.; Olivucci, M.; Robb, M. A.; Vreven, T. *J. Phys. Chem. A* **1997**, *101*, 3841.
(7) Dou, Y.; Allen, R. E. *J. Chem. Phys.* **2003**, *119*, 10658.
(8) Quenneville, J.; Martinez, T. J. *J. Phys. Chem. A* **2004**, *107*, 829.
(9) Improta, R.; Santoro, F.; Dietl, C.; Papastathopoulos, E.; Gerber, G. *Chem. Phys. Lett.* **2004**, *387*, 509.
(10) Dietl, C.; Papastathopoulos, E.; Niklaus, P.; Improta, R.; Santoro, F.; Gerber, G. *Chem. Phys.* **2005**, *310*, 201.
(11) Waldeck, D. H. *Chem. Rev.* **1991**, *91*, 415.
(12) Saltiel, J.; Sun, Y. P. In *Photochromism: Molecules and Systems*; Dürr, H., Bouas-Laurent, H., Eds.; Elsevier: Amsterdam, 1990; p 64.
(13) Görner, H.; Kuhn, H. J. *Adv. Photochem.* **1995**, *19*, 1.
(14) Meier, H. *Angew. Chem., Int. Ed. Engl.* **1992**, *31*, 13.
(15) Orlandi, G.; Gagliardi, L.; Melandri, S.; Caminati, W. *J. Mol. Struct.* **2002**, *612*, 383.
(16) Kwasnieswski, S. P.; Claes, L.; François, J.-P.; Deleuze, M. S. *J. Chem. Phys.* **2003**, *118*, 7823.
(17) Hohlneicher, G.; Wrzal, R.; Lenoir, D.; Frank, R. *J. Phys. Chem. A* **1999**, *103*, 8969.
(18) Hohlneicher, G.; Dick, B. *J. Photochem.* **1984**, *27*, 215.
(19) Syage, J. A.; Lambert, W. R.; Felker, P. M.; Zewail, A. H.; Hochstrasser, R. M. *Chem. Phys. Lett.* **1982**, *88*, 266.
(20) Orlandi, G.; Siebrand, W. *Chem. Phys. Lett.* **1975**, *30*, 352.
(21) Fuss, W.; Kosmidis, C.; Schmid, W. E.; Trushin, S. A. *Chem. Phys. Lett* **2004**, *385*, 423.
(22) Fuss, W.; Kosmidis, C.; Schmid, W. E.; Trushin, S. A. *Angew. Chem., Int. Ed.* **2004**, *43*, 4178.
(23) Saltiel, J.; Waller, A. S.; Sears, D. F. *J. Photochem. Photobiol., A* **1992**, *65*, 29.
(24) (a) Hudson, B. S.; Kohler, B. E. *J. Chem. Phys.* **1973**, *59*, 4984. (b) Tahara, T.; Hamaguchi, H. *Chem. Phys. Lett.* **1995**, *234*, 275.
(25) Abrash, S.; Repinec, S.; Hochstrasser, R. M. *J. Chem. Phys.* **1990**, *93*, 1041.
(26) Todd, D. C.; Fleming, G. R. *J. Chem. Phys.* **1993**, *98*, 269.
(27) Saltiel, J.; Ganapathy, S.; Werking, C. *J. Phys. Chem.* **1987**, *91*, 2755.
(28) Doany, F. E.; Heilweil, E. J.; Moore, R.; Hochstrasser, R. M. *J. Chem. Phys* **1984**, *80*, 201.
(29) Schneider, S.; Brem, B.; Jâger, W.; Rehaber, H.; Lenoir, D.; Frank, R. *Chem. Phys. Lett.* **1999**, *308*, 211.
(30) (a) Petersilka, M.; Gossmann, U. J.; Gross, E. K. U. *Phys. Rev. Lett.* **1996**, *76*, 1212. (b) M. K. Casida In *Recent Advances in Density Functional Methods, Part I*; Chong, D. P., Ed.; World Scientific: Singapore, 1995.
(31) (a) Adamo, C.; Barone, V. *J. Chem. Phys.* **1999**, *110*, 6158. (b) Enzerhof, M.; Scuseria, G. E. *J. Chem. Phys.* **1999**, *110*, 5029. (c) Perdew, J. P.; Burke, K.; Ernzerhof, M. *Phys. Rev. Lett.* **1996**, *77*, 3865,
(32) Frisch, M. J.; Trucks, G. W.; Schlegel, H. B.; Scuseria, G. E.; Robb, M. A.; Cheeseman, J. R.; Montgomery, J. A., Jr.; Vreven, T.; Kudin, K. N.; Burant, J. C.; Millam, J. M.; Iyengar, S. S.; Tomasi, J.; Barone, V.; Mennucci, B.; Cossi, M.; Scalmani, G.; Rega, N.; Petersson, G. A.; Nakatsuji, H.; Hada, M.; Ehara, M.; Toyota, K.; Fukuda, R.; Hasegawa, J.; Ishida, M.; Nakajima, T.; Honda, Y.; Kitao, O.; Nakai, H.; Klene, M.; Li, X.; Knox, J. E.; Hratchian, H. P.; Cross, J. B.; Bakken, V.; Adamo, C.; Jaramillo, J.; Gomperts, R.; Stratmann, R. E.; Yazyev, O.; Austin, A. J.; Cammi, R.; Pomelli, C.; Ochterski, J. W.; Ayala, P. Y.; Morokuma, K.; Voth, G. A.; Salvador, P.; Dannenberg, J. J.; Zakrzewski, V. G.; Dapprich, S.; Daniels, A. D.; Strain, M. C.; Farkas, O.; Malick, D. K.; Rabuck, A. D.; Raghavachari, K.; Foresman, J. B.; Ortiz, J. V.; Cui, Q.; Baboul, A. G.; Clifford, S.; Cioslowski, J.; Stefanov, B. B.; Liu, G.; Liashenko, A.; Piskorz, P.; Komaromi, I.; Martin, R. L.; Fox, D. J.; Keith, T.; Al-Laham, M. A.; Peng, C. Y.; Nanayakkara, A.; Challacombe, M.; Gill, P. M. W.; Johnson, B.; Chen, W.; Wong, M. W.; Gonzalez, C.; Pople, J. A. *Gaussian 03*, revision C.02; Gaussian, Inc.: Wallingford, CT, 2004.
(33) TURBOMOLE V5-7-1: (a) Ahlrichs, R.; Bär, M.; Häser, M.; Horn, H.; Kölmel, C. *Chem. Phys. Lett.* **1989**, *162*, 165. (b) Häser, M.; Ahlrichs, R. *J. Comput. Chem.* **1989**, *10*, 104. (c) Horn, H.; Weiss, H.; Häser, M.; Ehrig, M.; Ahlrichs, R. *J. Comput. Chem.* **1991**, *12*, 1058. (d) Treutler, O.; Ahlrichs, R. *J. Chem. Phys.* **1995**, *102*, 346. (e) Eichkorn, K.; Weigend,

F.; Treutler, O.; Ahlrichs, R. *Theor. Chem. Acc.* **1997**, *97*, 119. (f) Bauernschmitt, R.; Ahlrichs, R. *Chem. Phys. Lett.* **1996**, *256*, 454. (g) Weiss, H.; Ahlrichs, R.; Häser, M. *J. Chem. Phys.* **1993**, *99*, 1262. (h) Bauernschmitt, R.; Ahlrichs, R. *J. Chem. Phys.* **1996**, *104*, 9047. (i) Bauernschmitt, R.; Häser, M.; Treutler, O.; Ahlrichs, R. *Chem. Phys. Lett* **1997**, *264*, 573. (j) Grimme, S.; Furche, F.; Ahlrichs, R. *Chem. Phys. Lett* **2002**, *361*, 321. (k) Furche, F.; Ahlrichs, R. *J. Chem. Phys.* **2002**, *117*, 7433.

(34) Adamo, C.; Scuseria, G. E.; Barone, V. *J. Chem. Phys.* **2000**, *111*, 2889.

(35) Barone, V.; Cossi, M.; Tomasi, J. *J. Chem. Phys.* **1997**, *107*, 3210.

(36) Cossi, M.; Rega, N.; Scalmani, M.; Barone, V. *J. Chem. Phys.* **2001**, *114*, 5691.

(37) Cossi, M.; Barone, V. *J. Chem. Phys.* **2001**, *115*, 4708.

(38) Wiberg, K. B. *Tetrahedron* **1968**, *24*, 1083.

(39) (a) Foster, J. P.; Weinhold, F. *J. Am. Chem. Soc.* **1980**, *102*, 7211. (b) Reed, A.; Weinhold, F. *J. Chem. Phys.* **1983**, *78*, 4066. (c) Glendening, E. D.; Weinhold, F. *J. Comput. Chem.* **1998**, *19*, 593.

(40) Traetteberg, M.; Frantsen, E. B.; Mijlhoff, F. C.; Hoekstra, A. *J. Mol. Struct.* **1975**, *26*, 57.

(41) Jovanovic, J.; Schiûrmann, M.; Preut, H.; Spiteller, M. *Acta Crystallogr.* **2001**, *E*57, o1100.

(42) Jovanovic, J.; Elling, W.; Schûrmann, M.; Preut, H.; Spiteller, M. *Acta Crystallogr.* **2002**, *E*58, o35.

(43) Todd, D. C.; Fleming, G. R.; Jean, J. M. *J. Chem. Phys.* **1992**, *97*, 8915.

(44) Saltiel, J.; Waller, A. S.; Sears, D. F., Jr. *J. Am. Chem. Soc.* **1993**, *115*, 2453.

(45) (a) Greene, B. I.; Farrow, R. C. *J. Chem. Phys.* **1983**, *76*, 336. (b) Baumert, T. *Appl. Phys. B* **2001**, *72*, 105. (c) Pederson, S.; Banares, L.; Zewail, A. H. *J. Chem. Phys.* **1992**, *97*, 8801.

(46) (a) Syage, J. A.; Felker, P. M.; Zewail, A. H. *J. Chem. Phys.* **1984**, *81*, 4706. (b) Baskin, J. S.; Banares, L.; Pedersen, S.; Zewail, A. H. *J. Phys. Chem.* **1996**, *100*, 11920.

(47) Amirav, A.; Jortner, J. *Chem. Phys. Lett.* **1982**, *95*, 295.

(48) Matousek, P.; Parker, A. W.; Phillips, D.; Scholes, G. D.; Toner, W. T.; Towrie, M. *Chem. Phys. Lett.* **1997**, *278*, 56.

(49) Warshel, A. *J. Chem. Phys.* **1975**, *62*, 214.

(50) Nikowa, L.; Schwarzer, D.; Troe, J.; Schroeder, J. *J. Chem. Phys.* **1992**, *97*, 4827.

(51) (a) Petek, H.; Yoshihara, K.; Fujiwara, Z.; Lin, J. H.; Penn, J. H.; Frederick, J. *J. Chem. Phys.* **1990**, *94*, 7539. (b) Petek, H.; Fujiwara, Z.; Kim, K.; Yoshihara, K. *J. Am. Chem. Soc.* **1988**, *110*, 6269.

(52) (a) Muszkat, K. A.; Fisher, E. *J. Chem. Soc. B* **1967**, 662. (b) Gegiou, G.; Muszkat, K. A.; Fisher, E. *J. Am. Chem. Soc.* **1967**, *90*, 12.

(53) Ishii, K.; Takeuchi S.; Tahara, T. *Chem. Phys. Lett.* **2004**, *398*, 400.

(54) Banares, L.; Heikal, A. H.; Zewail, A. H. *J. Phys. Chem.* **1992**, *96*, 4127.

(55) Maitra, N. T.; Zhang, F.; Cave, R. J.; Burke, K. *J. Chem. Phys.* **2004**, *120*, 5932.

(56) Oelgemoller, M.; Brem, B.; Frank, R.; Schneider, S.; Lenoir, D.; Hertkorn, N.; Origane, Y.; Lemmen, P.; Lex, J.; Inoue, Y. *J. Chem. Soc., Perkin Trans. 2* **2002**, 1760.